

References and Notes

1. A. O. Nier, W. B. Hanson, A. Seiff, M. B. McElroy, N. W. Spencer, R. J. Duckett, T. C. D. Knight, W. S. Cook, *Science* **193**, 786 (1976).
2. A. Seiff, *Space Sci. Instrum.*, in press.
3. A. O. Nier, W. B. Hanson, M. B. McElroy, A. Seiff, N. W. Spencer, *Icarus* **16**, 74 (1972).
4. P. Gierasch and R. Goody, *Planet. Space Sci.* **16**, 615 (1968).
5. The fact that the atmospheric pressure curve passes near the measured values during descent engine operation is probably fortuitous.
6. Viking Meteorology Team, personal communication.
7. An order of magnitude estimate shows that the pressure difference between the sites cannot be accounted for by dynamics. Pressure differences due to measured wind velocities are on the order of 10^{-3} mbar.
8. It is now clear that this reference level cannot be identified with a specified atmospheric pressure, since pressure varies seasonally [S. L. Hess *et al.*, *Science* **194**, 78 (1976)]. By chance, pressure at the reference ellipsoid was 6.14 mbar (from Viking 1 data) on 3 September 1976.
9. T. Owen and K. Biemann, *Science* **193**, 803 (1976).
10. R. W. Zurek, *J. Atmos. Sci.* **33**, 321 (1976).
11. J. L. Elliot, R. G. French, E. Dunham, P. J. Gierasch, J. Veverka, C. Church, C. Sagan, *Science*, in press.
12. H. H. Kieffer, S. C. Chase, Jr., D. D. Miner, F. D. Palluconi, G. Münch, G. Neugebauer, T. Z. Martin, *ibid.* **193**, 780 (1976).
13. A. O. Nier, personal communication.
14. E. J. Christensen, *J. Geophys. Res.* **80**, 2909 (1975).
15. Radio tracking radius (personal communication from E. Euler of the Viking Flight Team).
16. Radius from measured acceleration due to gravity (personal communication from E. J. Christensen).
17. The authors extend their appreciation to S. Cook of the Viking Entry Science team and to E. Euler, F. Hopper, R. Dupree, and others of the Viking Flight Team who provided invaluable support. Thanks also are due to many colleagues at Ames Research Center, in particular S. Rogallo for computer programming support and to S. C. Sommer for support during the mission operations period. The authors are further indebted to C. B. Leovy for helpful discussions on the thermal tidal processes.

18 October 1976

Viking Magnetic Properties Investigation: Further Results

Abstract. *The amounts of magnetic particles held on the reference test chart and backhoe magnets on lander 2 and lander 1 are comparable, indicating the presence of an estimated 3 to 7 percent by weight of relatively pure, strongly magnetic particles in the soil at the lander 2 sampling site. Preliminary spectrophotometric analysis of the material held on the backhoe magnets on lander 1 indicates that its reflectance characteristics are indistinguishable from material within a sampling trench with which it has been compared. The material on the RTC magnet shows a different spectrum, but it is suspected that the difference is the result of a reflectance contribution from the magnesium metal covering on the magnet. It is argued that the results indicate the presence, now or originally, of magnetite, which may be titaniferous.*

The aim of the Viking magnetic properties investigation (1) is to estimate the abundance and composition of magnetic minerals in the martian surface material at the Viking landing sites. Two magnet arrays in the surface sampler backhoe enter the surface material during sample acquisition and attract and hold any magnetic particles present. Another array mounted on one of the imaging reference test charts (RTC) on top of each lander attracts magnetic particles already in, or raised into, the Martian atmosphere.

Details of the magnet arrays have been given by Hargraves *et al.* (2). Briefly, each array consists of a cylindrical magnet surrounded by, and separated from, a ring magnet. The overall dimensions of each array are 1.8 cm diameter and 0.3 cm thick, and the central and ring magnets are oppositely magnetized along their axes. Two arrays are placed in the backhoe in such a way that their surfaces are respectively 0.5 mm and 3.0 mm below the backhoe surface on one side and 3.0 mm and 0.5 mm below on the other; thus, at each face of the backhoe there are two levels of attractive force, in the approximate ratio of 12 : 1. Images of the backhoe are periodically taken by the lander cameras, the back face directly

and the front by way of a $4\times$ magnifying mirror. The RTC magnet is a single array equivalent to a strong backhoe array.

Results from Viking 1. Results from Viking 1 (VL1), based on images received up to sol 34, have already been described (2) and are summarized here.

After initially attracting some particles out of the dust cloud raised by the terminal descent engines during the final stages of the landing, the magnet on the RTC attracted considerably more material during the mission, indicated by a well-defined bull's-eye pattern of particles over the magnet array. The chief source of this material is believed to be dust raised by surface sampling activity and subsequent distribution of the soil samples to the three analytical experiments. There may also be a contribution from magnetic particles attracted from the martian atmosphere.

The backhoe magnets attracted a considerable quantity of relatively low albedo magnetic particles from the soil during surface sampling activity, including one or two small fragments 2 to 3 mm across. The existence of well-defined bull's-eye patterns of similar extent on both strong and weak magnets indicated the presence in the soil of a strongly mag-

netic, relatively pure mineral. This was considered most likely to be magnetite, and by comparison with laboratory tests on terrestrial materials its abundance was estimated as 3 to 7 percent by weight.

On sol 40, a high resolution, direct view image of the backhoe was received, after a cumulative total of 13 insertions into the surface. This image indicates that slightly more material was held on sol 40 than on sol 28, and that some millimeter-sized fragments were still adhering on sol 40.

On sol 41, further images of the backhoe were received that were taken during a special sequence in which insertion of the backhoe into the surface was followed by imaging, by way of the magnifying mirror, the material held on the front of the backhoe both before and after vibration. Considerably more material was held on the magnets before than after vibration of the collector head, indicating that much non- or weakly magnetic material entrained with the strongly magnetic particles was purged by this vibration.

A list of images of the RTC and backhoe magnets received since sol 34 is given in Table 1. [For a list of previous images received, see (2).]

Results from Viking 2: The RTC magnet. A low resolution image made in the survey mode on Viking 2 (VL2) on sol 0, in which no clear bull's-eye pattern can be discerned, and a high resolution image on sol 6 were received before any sampling activity had occurred (Fig. 1a). In the sol 6 image there was significantly more material on the magnet than was observed on the Viking 1 magnet at the nearest corresponding time (sol 3). This could have been the result of a relatively larger or denser dust cloud which might have been raised during the landing of VL2 because of an extra burn of the terminal descent engines just before touchdown. It is believed that the material was not seen in the sol 0 image of the magnet because of its small size and the lack of contrast. A comparison of the material held on the RTC magnets on sol 15 (VL1) and sol 13 (VL2) shows somewhat less material held on the latter than the former. On both landers there was sampling activity on sol 8, but because of an anomaly on the surface sampler only one delivery had occurred on VL2 as opposed to four on VL1. This difference probably explains the above observations.

A further comparison of the RTC magnets on the two landers can be made for sols 31 (VL1) and 33 (VL2). After a simi-

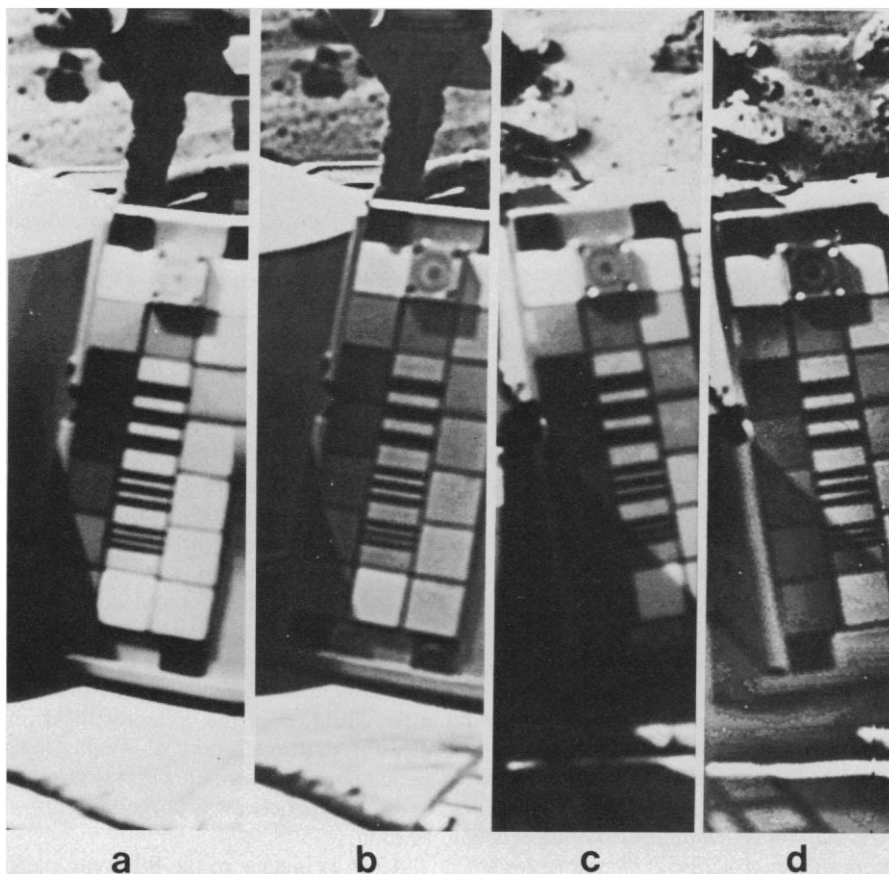


Fig. 1. The RTC magnet as seen on sol 6 (a), sol 13 (b), sol 33 (c), and sol 42 (d). Images (a) and (b) were taken with camera 1, (c) and (d) with camera 2. These images clearly show the increase in the density of the bulls'-eye pattern of adhering particles between sols 6 and 13. The apparent increase after sol 13 may be an artifact of image processing and geometry, because the two pairs of pictures were taken with different cameras. A thorough analysis with the raw digital data is in progress.

lar total number of sample deliveries (six on VL1, five on VL2) the VL2 magnet still had somewhat less material adhering to it compared with that on VL1. The significance of this observation is difficult to assess; variables include wind speed and direction during sampling and delivery, and grain size distribution and magnetic mineral content of the samples.

As described below, the evidence from the backhoe magnets is that the content of magnetic particles in the surface at the two landing sites is comparable. The grain size at the Bonneville and Beta sites may be somewhat coarser than at Sandy Flats at the VL1 site (3), but we think that neither the relative abundance, nor the particle size, can cause the differences observed.

Meteorological data obtained on 20 sols from each lander were averaged, and the results indicate that the wind directions are variable at both sites (4). At the VL1 site, the winds blew from between SE and SW during the times of sampling activity, tending to transport dust raised into the atmosphere by this activity toward the RTC magnet. At the landing site of VL2, the prevailing winds during sampling periods blew from between SW and NW, tending to blow raised dust away from the RTC magnet.

If atmospheric particles are being attracted, the number held will also be dependent on the average speed and direc-

Table 1. Magnet images received from Viking 1. This table continues Table 1 in (2). The image reference number consists of, first, the camera event number and, second, the roll and frame number, the frame number of the best image being given. Survey refers to low-resolution camera mode; HR, high-resolution camera mode. All color and infrared pictures are low resolution. Direct view is view of the back surface of backhoe.

Sol	Image reference No.	RTC magnet	Backhoe magnets	Comments
36	12B054/036		HR, shade	Direct view after 11th sample acquisition: out of focus
38	12B067/038		HR, sun	Direct view, out of focus
	F1045/36			
39	11B073/039	HR, shade		Out of focus
	F1046/60			
40	11B088/040	Color, infrared, survey, shade		
	F1047/67			
40	11B092/040		Color, infrared, sun	First color image of backhoe
	F1047/8			
40	11B093/040		HR, sun	Direct view after 13th sample acquisition
	F1047/14			
40	11B099/040	HR, sun		Out of focus
	F1048/20			
41	12B104/041		HR, sun	Front of backhoe $\times 4$ mirror; after insertion into surface, before vibration
	F1049/7			As above
41	12B105/041		Color	As above
	F1049/12			
41	12B106/041		HR, sun	As above, after vibration
	F1049/19			
41	12B107/041	Color, sun	Color, sun	Combined image of backhoe and RTC magnet
	F1049/24			
41	12B112/041	HR shadow		Out of focus
	F1049/68			
57	12B141/057	Color, shade		
	F1056/20			
76	12B166/076	Color, shade		
	F1063/12			

tion of the wind at each site, and also on the number density of the particles. There is evidence from the atmospheric extinction coefficients at the two sites, 0.35 and 0.25 at VL1 and VL2, respectively, that there are fewer atmospheric particles at the VL2 site, if one assumes a similar size distribution (5). Also, the prevailing winds at the two sites would tend to favor particle capture by the RTC magnet on VL1 rather than VL2. Because of these observations, we believe that the difference in the amount of material adhering to the RTC magnets reflects different wind conditions during sample acquisition and delivery, and possibly also indicates the presence of less very fine-grained material at the VL2 than at the VL1 site (3). This, if true, would imply that less dust persists in the atmosphere and drifts over the RTC magnet during the delivery procedure on VL2.

During the extended mission, there will be an opportunity for imaging the RTC magnets on both landers after long intervals during which there will have been little or no sampling activity. Any changes observed in the material on the magnets will presumably be due to acquisition of dust from the atmosphere or its removal by wind, or a combination of both of these effects. Significant removal of the material by winds would indicate a weakly magnetic mineral, most probably goethite or hematite, both of which are candidate minerals for atmospheric particles. Any strongly magnetic minerals (see Fig. 2) would not be removed in this way.

Backhoe magnets. The first good image of the VL2 backhoe was received on sol 28 (Fig. 3a) after three insertions of the backhoe into the surface and subsequent vibration during sample delivery and purge. Each magnet is well covered with particles, both weak and strong bull's-eye patterns being very similar in size and intensity, as in the images from VL1. This again suggests the presence of a relatively pure magnetic mineral in the surface material at the VL2 site. Subsequent images obtained during sample acquisitions and rock-moving activities on sols 29, 30, 33, 36, and 45 (see Table 2) confirmed the above observations. The later images suggested that the magnets were near saturation, in that there appeared to be a more or less constant amount of material held. However, further images received on sol 46 and 47 after additional sample acquisitions at the Beta site (3), showed evidence of considerably more material on each magnet. These later images were taken when the sun was at an angle of about 15° relative to the backhoe surface (Fig. 3b), and the

extent of the shadow suggests a particle pile 2 to 4 mm high. These images were received after the backhoe had been in the surface 9 times (including 3 in-

sertions at the Beta sampling site) on sol 46, and 11 times (including 5 insertions at the Beta site) on sol 47. Because the image on sol 45 is too far out of focus, the

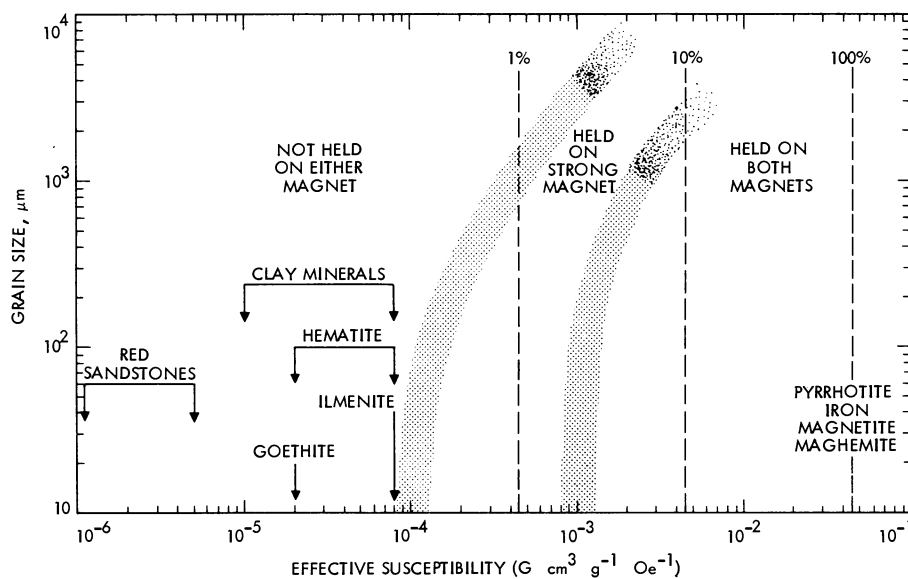


Fig. 2. Diagram illustrating the response to the backhoe magnets of the common magnetic minerals, according to their grain size and magnetic susceptibility. The diagram is based on extrapolation of the results of laboratory experiments (with Viking backhoe magnets and natural and synthetic materials) to the conditions which we consider to apply when the magnets are actually deployed during sampling activity on Mars. The vertical broken lines refer to composite particles containing different percentages of any of the four strongly magnetic minerals. The broad stippled bands separate the three main levels of magnetic attraction between which there is no clear division. (G, gauss; Oe, oersted.)

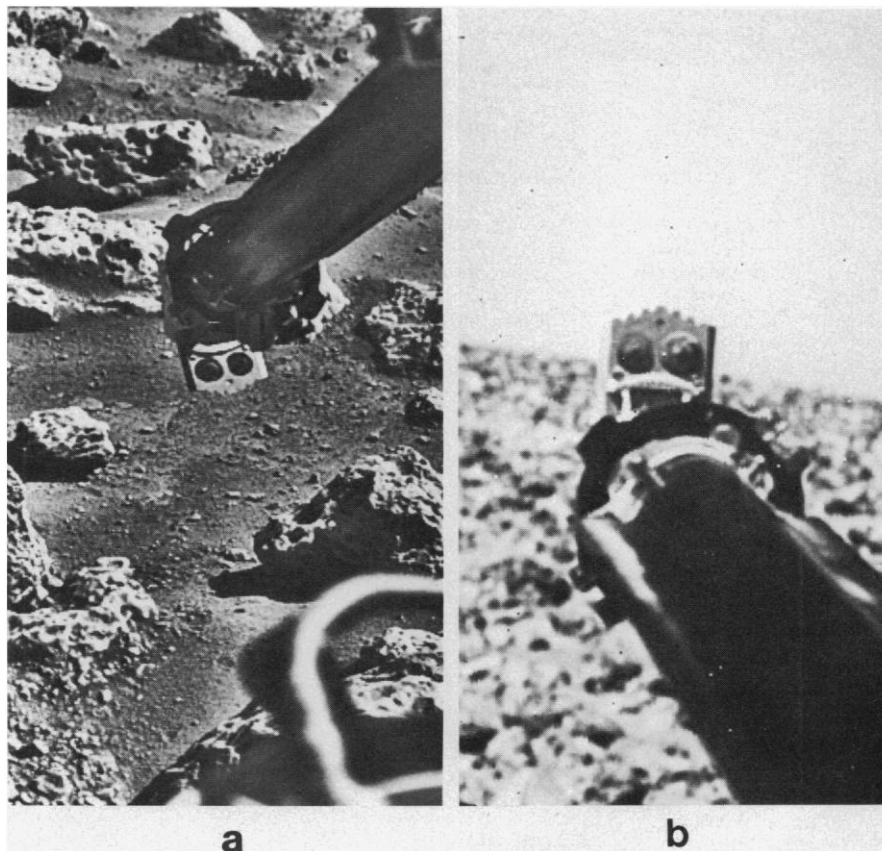


Fig. 3. Direct view images of the backhoe after a total of three insertions (a) and 11 insertions (b) into the surface. Note the similar amount of material adhering to both strong and weak magnets: in (a) the weak magnet is to the right and in (b) to the left.

best previous image obtained of the backhoe after insertion at the Beta site was on sol 28 (after 2 insertions). The adhering material appears to be relatively much less in this earlier picture, but on sol 28 the sun angle was greater (about 45°), so shadows were unlikely to be cast and the contrast may not be so marked. We tentatively conclude that there is a greater concentration of magnetic particles at the Beta site (3) compared with the other sampling sites, and it is hoped that this result may be further investigated during the Viking extended mission.

On sol 56, an image of the backhoe was received showing two small (2 to 3 mm) fragments held by the strong magnet. These fragments appear to have

been extracted from the soil during the biology sample acquisition from under "Notch" rock (3) on sol 51, and are similar in size to those attracted to the VL1 backhoe magnets (2). After a further insertion into the surface, these or other similar-sized fragments can still be seen on the magnets.

Spectrophotometric analysis. The lander cameras have six channels for use in defining spectral reflectivity in the wavelength range from 0.4 to 1.1 μm . Because of signal-to-noise constraints, the channels were constructed with interference filters with bandwidths of approximately 0.1 μm (6). Three of the channels have appreciable out-of-band response. Because of the nature of the channels it is difficult to assign each an

effective wavelength and then to plot wavelength against reflectance; this is especially true for two of the infrared (IR) channels (7). An alternative method of data reduction has been developed, however, that utilizes the channel responsivity functions and their out-of-band signals to advantage by treating reflectivity as a linear sum of basic functions embedded in the integral that defines the channel preamplifier voltage (8).

A preliminary comparison of the reflectivity of material clinging to the magnets can, however, be derived by utilizing the blue, green, red, and IR 1 channels as discrete wavelengths (9, 10). More refined analyses are in progress. Although treating the channels as having effective wavelengths degrades the re-

Table 2. Magnet images received from Viking 2. The image reference number consists of, first, the camera event number and, second, the roll and frame number, the frame number of the best image being given. Survey refers to low-resolution camera mode; HR, high-resolution camera mode. All color and infrared pictures are low resolution. Direct view is view of the back surface of backhoe.

Sol	Image reference No.	RTC magnet	Backhoe magnets	Comments
0	22A002/000 F2001/39	Survey, sun		
6	21A040/006 F2013/20	HR, sun		Before any sampling activity
10	21A076/010 F2019/2		HR, shade	Out of focus, after first sample acquisition (Beta site)
12	22A086/012 F2021/47		Survey, shade	Out of focus, after first sample acquisition (Beta site)
12	21A081/012 F2021/21	Color, sun		First color image
13	21A090/013 F2022/20	HR, sun		
16	21A120/016 F2025/10	Survey, shade		
18	21A129/018 F2026/3	HR, sun		Out of focus
21	22A160/021 F2030/39	Color, infrared, shade		
22	22A166/022 F2031/46	Color, sun		
23	22A181/023 F2034/7	Color, infrared, survey, shade		
23	21A184/023 F2034/14	Color, infrared, survey, shade		
24	21A196/024 F2035/12	Color, sun		
25	21A204/025 F2035/40	HR, sun		Out of focus
25	21A212/025 F2035/102	Color, infrared		
28	21A229/028 F2039/38		HR, sun	After a total of three sample acquisitions
29	22A239/029 F2040/32		HR, sun	Weak magnet visible only
29	21A241/029 F2040/40		HR, shade	
30	21A246/030 F2040/56		HR, sun	After a total of four sample acquisitions
30	21A248/030 F2040/64		HR, sun	Long range, direct view images taken during rock moving activity
30	21A249/030 F2040/68		HR, sun	As above
30	21A250/030 F2040/72		HR, sun	As above
33	22B020/033 F2043/19	HR, sun		
33	21B022/033 F2043/15		HR, sun	Magnets partially shadowed

flectivity estimate, it does serve to delineate similarities and differences. Effective wavelengths for these channels are 0.500, 0.556, 0.669, and 0.867 μm , respectively (7).

Figure 4 shows estimated reflectance values for material on the backhoe magnet, for material on the reference test chart magnets, and for the bare magnesium cover on the RTC magnet (11). Also plotted is the reflectance for a portion of the trench imaged on sol 26 (11). Note that these reflectivities are actually a product of normal albedo and the photometric function, that is, lighting and viewing geometry effects on reflectivity have not been taken into account numerically.

Nevertheless, some preliminary observations can be made. First, the material on the two backhoe magnets is spectrally

indistinguishable to the accuracy that can be discerned by the technique of data reduction used. Second, the material on the backhoe magnets is similar to the material in the trench. The particular region chosen for reflectivity of the trench has lighting and viewing angles similar to the backhoe images, thus reducing brightness differences due to lighting and viewing geometry. Third, the material on the RTC magnets is either spectrally distinct from the other materials or the magnesium cover on the magnets composes part of the observed brightness. We favor the latter interpretation, pending the results of experiments in progress designed to measure more accurately the reflectance of the bare RTC magnet.

Discussion. The appearance of both RTC and backhoe magnets at VL2 up to

sol 47, is very similar to that at an equivalent time at VL1 (sol 41), and hence we would infer a similar abundance of relatively pure magnetic particles, 3 to 7 percent by weight (2). There was some indication of a variation in the abundance between the Alpha and Beta sites (3), however, and these estimates of magnetic mineral abundance are tentative. In the extended mission it is planned to clean the magnets with the cleaning brush and perform specific experiments to refine the abundance estimate at the two landing sites. However, the meaning of the present estimate, the possible identity of the magnetic mineral particles, and their potential significance are discussed below.

Purity of magnetic particles. The susceptibility and saturation magnetization of the common strongly magnetic miner-

(Table 2 continued)

Sol	Image reference No.	RTC magnet	Backhoe magnets	Comments
34	22B027/034 F2044/28	Color, sun		
36	22B041/036 F2047/74		HR, sun	After a total of six insertions into surface
36	22B045/036 F2047/84		HR, shade	
36	21B043/036 F2047/78	Color, sun		
42	22B101/042 F2053/7	Color, shade		
42	22B098/042 F2052/34	HR, sun		
43	21B104/043 F2054/5	Color, shade		
44	22B111/044 F2054/51	Color, infrared, survey, sun		
45	21B121/045 F2055/24		HR, part shaded	After a total of eight insertions into the surface
46	22B129/046 F2056/37	Color, infrared, survey, sun		
46	22B136/046 F2057/20		Color, infrared, survey, sun	First color image of material on backhoe; total of nine insertions
47	22B146/047 F2058/47		HR, sun	After a total of 11 insertions into the surface
48	22B151/048 F2058/64	Color, infrared, survey, sun		
49	22B180/049 F2059/51	Color, infrared survey, sun		
50	22B190/050 F2060/104	Color, infrared survey, sun		
51	21B203/051 F2061/4		HR, shade	After total of 13 insertions into the surface
51	22B207/051 F2061/21	Color, infrared, sun		
56	22C021/056 F2067/20		HR, sun	Front of backhoe in \times 4 mirror
56	22C022/056 F2067/24		HR, sun	Direct view, before insertion
56	22C026/056 F2067/40		HR, sun	Direct view, after total of 14 insertions into surface, after vibration
56	22C030/056 F2067/56		HR, sun	Front of backhoe in \times 4 mirror
57	22C037/057 F2067/83	Color, infrared	Color, infrared	Combined image of backhoe and RTC magnet
57	22C039/057 F2067/94	HR, shade	HR, sun	As above

als are so high, that the admixture even of as little as 1 percent magnetite (or equivalent) in an otherwise nonmagnetic 100- μm particle enhances its susceptibility to the extent that it will be attracted to the strong Viking magnets (Fig. 2). But if the apparently magnetic particles were generally composite, and the concentration of the truly magnetic phase were low in each particle, there would usually be a marked difference in response between the weak and strong magnet arrays of the backhoes. After five or more insertions into the surface, the appearance of the two backhoe magnets at both landing sites has, on the contrary, been remarkably similar. It is this which prompts the inference of relative purity for the magnetic particles at both sites. From experiments with natural terrestrial samples, the clear contrast in the response between weak and strong magnets begins to disappear if the particles contain more than 25 percent of the highly magnetic phase (usually magnetite). Thus, our preliminary abundance estimate of 3 to 7 percent by weight of "relatively pure" magnetic particles could be consistent with the presence in the soil of as little as 1 percent Fe_3O_4 or $\gamma\text{-Fe}_2\text{O}_3$ equivalent. If they are not altogether pure, the estimated minimum of 3 percent magnetic particles could consist of an admixture with silicates, or with other nonmagnetic oxide phases. The admixture could, for example, be a solid solution of ulvöspinel (Usp) with magnetite (Mt) or an oxidized magnetite-ilmenite intergrowth. It is interesting to note that if the magnetic particles on Mars are titaniferous magnetite (or titanomaghemite) containing 20 percent TiO_2 (equivalent to about $\text{Usp}_{60}\text{Mt}_{40}$), then an abundance of about 5 percent would more than suffice to explain the 0.85 percent TiO_2 in the martian soil (12).

There is, however, no evidence of whether or not the TiO_2 content of the soil is closely associated with the magnetic particles. No means of implementing on Mars an analysis of the magnetic particles themselves or, alternatively, of the soil with the magnetic fraction removed, has yet been devised.

Composition of particles. The spectrophotometric data available at present for the magnetic particles clinging to the backhoe magnet show them to be red and essentially indistinguishable from the martian surface material as exposed in the trenches. This corrects our original inference that the magnetic particles were darker (2) than the average surface material. To the extent that the color of the martian surface is attributed to ferric iron in the form of limonite or hematite,

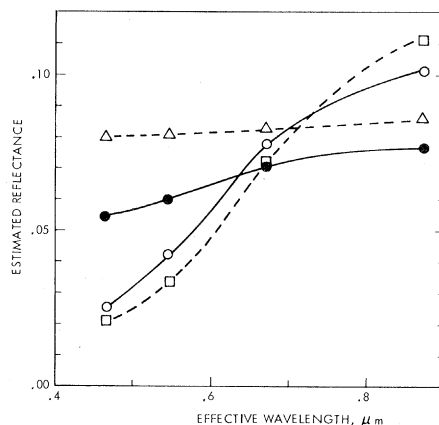


Fig. 4. Estimated reflectance plotted against effective wavelength for the material on the VLI RTC magnet (closed circles), VLI backhoe magnets (open circles) and for the trench in Sandy Flats (3) as imaged on sol 26 (open squares). Reflectance values from the magnesium cover over the magnet are also shown (open triangles).

both of which are nonmagnetic (Fig. 2), these results give no clue as to the composition of the magnetic particles or the truly magnetic component of them.

The particles could, conceivably, be composed of pure maghemite, $\gamma\text{-Fe}_2\text{O}_3$; the color of this mineral, however, is not well known. A synthetic sample of $\gamma\text{-Fe}_2\text{O}_3$ (13) is yellow-brown, rather than red, but in nature the color is probably highly variable.

Alternatively, the magnetic particles could consist of a core of any one of the three other candidates (2) (iron, magnetite, pyrrhotite) with a thin coating of reddish hematite or limonite. The only hope of resolving this uncertainty directly lies in the more complete spectrophotometric analyses currently being made.

Origin of magnetic particles. In addition to hematite, $\alpha\text{-Fe}_2\text{O}_3$, maghemite has been reported to result from the photostimulated oxidation of magnetite under martian conditions (14). In addition to direct, low-temperature oxidation of magnetite to maghemite, the latter also forms by the dehydration of lepidocrocite, $\gamma\text{-FeO.OH}$ in contrast to goethite, $\alpha\text{-FeO.OH}$, which dehydrates to hematite, $\alpha\text{-Fe}_2\text{O}_3$ (15). Goethite (possibly together with lepidocrocite) is the principal component of limonite.

If the magnetic mineral on Mars is maghemite formed by low-temperature oxidation of magnetite (titaniferous or otherwise) the petrogenetic significance associated with the original presence of magnetite will still apply. If, on the other hand, the maghemite formed by dehydration of lepidocrocite, which was a component of limonite formed by alteration of ferroan silicates, then magnetite is not a necessary precursor. Experi-

ments utilizing magnetic property measurements are planned to test the extent of lepidocrocite production in connection with the oxidation and hydration of Fe bearing silicates under martian conditions. On Earth, however, most maghemite is apparently derived ultimately from magnetite (15). Thus, the magnetic particles present in the surface material of Mars at the two Viking landing sites can be considered to reflect at least the original presence of magnetite, even if none is now preserved. The extent of the possible oxidation to maghemite cannot be determined.

Possible implications. The interpretation of the magnetic particles on Mars as indicating, directly or indirectly, the original presence of magnetite, has a variety of implications.

Magnetite, per se, is not an equilibrium product of weathering under martian conditions (16); hence, if present, it was most likely derived from some pre-existing igneous or metamorphic rock. Earth-based spectral reflectance studies of Mars (17) are interpreted to signify that the dark areas are composed of relatively less-oxidized basalt, containing considerable FeO. The light areas on the other hand are interpreted as being more oxidized, low in FeO relative to ferric iron, and rich in clay alteration products.

If the magnetite is pyrogenic, and derived from breakdown of an extrusive igneous rock, such as basalt, then by terrestrial analogy one would expect it to be titaniferous. On the other hand, if the magnetite is produced by metamorphism or deuteritic alteration (serpentinization, for example), then it is probably low in TiO_2 .

These arguments emphasize the desirability of determining whether or not the TiO_2 of the martian fines is closely associated with the magnetic fraction. Every effort will be made in the extended mission to implement an experiment to test this possibility.

R. B. HARGRAVES

Department of Geological and Geophysical Sciences, Princeton University, Princeton, New Jersey 08540

D. W. COLLINSON

Institute of Lunar and Planetary Sciences, School of Physics, University of Newcastle upon Tyne, Newcastle upon Tyne, England

R. E. ARVIDSON

McDonnell Center for the Space Sciences, Department of Earth and Planetary Sciences, Washington University, St. Louis, Missouri 63160

C. R. SPITZER

NASA Langley Research Center, Hampton, Virginia 23665

References and Notes

- R. B. Hargraves and N. Petersen, *Icarus* **16**, 223 (1972).
- R. B. Hargraves, D. W. Collinson, C. R. Spitzer, *Science* **194**, 84 (1976).
- R. W. Shorthill, H. J. Moore, R. E. Hutton, R. F. Scott, C. R. Spitzer, *ibid.*, p. 1309.
- S. L. Hess, R. M. Henry, C. B. Leovy, J. A. Ryan, J. E. Tillman, T. E. Chamberlain, H. L. Cole, R. G. Dutton, G. C. Greene, W. E. Simon, J. L. Mitchell, *ibid.* **194**, 78 (1976); S. L. Hess, personal communication.
- T. Mutch, S. Grenander, K. Jones, W. Patterson, R. Arvidson, E. Guinness, P. Avrin, E. Carlston, A. Binder, C. Sagan, E. Dunham, P. Fox, D. Pieri, F. Huck, C. Rowland, G. Taylor, S. Wall, R. Kahn, E. Levinthal, S. Liebes, R. Tucker, E. Morris, J. Pollack, R. Saunders, M. Wolf, *Science* **194**, 1277 (1976).
- F. O. Huck, H. F. McCall, W. R. Patterson, G. R. Taylor, *Space Sci. Instrum.* **1**, 189 (1975).
- L. Kelly, F. O. Huck, R. E. Arvidson, NASA TN-X-72778 (1975).
- S. Park and F. O. Huck, *Appl. Opt.*, in press.
- Reflectance can be derived by normalizing the preamplifier voltage for each channel to the voltage obtained for each channel for one of the reference test chart patches mounted on the lander.

$$\frac{V_{1,m}}{V_{1,RTC}} = \frac{C_1 \int_0^\infty \tau_1(\lambda) \rho(\lambda)_m \phi_m(i, e, g, \lambda) d\lambda}{C_1 \int_0^\infty \tau_1(\lambda) \rho(\lambda)_{RTC} \phi_{RTC}(i, e, g, \lambda) d\lambda} \quad (1)$$

where $V_{1,m}$ is the preamplifier voltage for the i th channel imaging the magnetic material, $V_{1,RTC}$ is the equivalent for imaging one of the test patches, C_1 is a channel-dependent calibration constant, and $\tau_1(\lambda)$ is the channel dependent transfer function, which is the product of the camera optical throughput, solar irradiance, atmospheric transmittance, and photosensor responsivity; $\rho(\lambda)_m$ is the normal albedo of the magnetic material, and $\phi_m(i, e, g, \lambda)$ is its photometric function, where i is the incidence angle, e is the emission angle, g is the phase angle, and λ is the wavelength. $\rho(\lambda)_{RTC}$ and $\phi_{RTC}(i, e, g, \lambda)$ are the corresponding functions for one of the test patches. Since the test patches have a Lambertian photometric function (I_0), and since the blue, green, red, and IR 1 channels can be approximated as single wavelength samples, this equation reduces to:

$$\frac{\rho(\lambda)_{1,m} \phi_{1,m}(i, e, g, \lambda)}{V_{1,RTC}} = \frac{V_{1,m}}{V_{1,RTC}} \rho(\lambda)_{RTC} \cos i \quad (2)$$
- Gray patch reflectances of the RTC have been measured over a wide range of lighting and viewing geometry. The ratio of measured reflectance to that of an ideal Lambertian scatterer deviates from unity by no more than ± 10 percent. (A Lambertian surface scatters light equally in all directions.) In addition, the gray patch reflectances are not strongly wavelength dependent [see S. Wall, E. Burcher, D. Jobson, NASA TN-C-72762 (1975)]. Note that an additional error associated with radiometric calibration with the test patches is that they are located atop the lander and hence may receive reflected light from parts of the lander structure. This impairs the accuracy of absolute radiometric calibration since $\tau_1(\lambda)$ is then different for the numerator and denominator in Eq. 1 (9). Since the lander is painted with spectrally flat material, light reflected from the lander probably only serves to change the denominator by some constant. Problems do arise, however, in directly comparing the RTC and backhoe magnets since one is near the martian surface and one near the spacecraft. Analysis is underway to estimate the magnitude of lander-reflected light.
- The backhoe image used was 11B040/040. For this image $i = 55^\circ$, $e = 20^\circ$, $g = 65^\circ$. RTC magnet images were 12B032/034 and 12B069/039. RTC magnet reflectivities were nearly identical. For these images $i = 73^\circ$, $e = 21^\circ$, $g = 78^\circ$. The trench image was 11A147/026, and $i = 60^\circ$, $e = 25^\circ$, $g = 65^\circ$. Values for the trench lighting and viewing angles are only known to 20 percent because of uncertainties in the trench topography.
- B. C. Clark, A. K. Baird, H. J. Rose, P. Toulmin, K. Keil, A. Castro, W. Kelliher, C. Rowe, P. Evans, *Science* **194**, 1284 (1976).
- Sample provided by K. S. Deffeyes.
- R. L. Huguenin, *J. Geophys. Res.* **78**, 8481 (1973).
- W. A. Deer *et al.*, *Rock Forming Minerals*, (Wiley, New York, 1962), vol. 5.
- J. T. O'Connor, *J. Geophys. Res.* **73**, 5301 (1968).
- J. B. Adams and T. B. McCord, *ibid.* **74**, 4851 (1969).
- Supported in part by the NASA Langley Research Center. We acknowledge with thanks the assistance of the Surface Sampler and Lander Imaging Teams in obtaining the pictures of the magnetic arrays on which our interpretations are based.

15 November 1976

The Environs of Viking 2 Lander

Abstract. *Forty-six days after Viking 1 landed, Viking 2 landed in Utopia Planitia, about 6500 kilometers away from the landing site of Viking 1. Images show that in the immediate vicinity of the Viking 2 landing site the surface is covered with rocks, some of which are partially buried, and fine-grained materials. The surface sampler, the lander cameras, engineering sensors, and some data from the other lander experiments were used to investigate the properties of the surface. Lander 2 has a more homogeneous surface, more coarse-grained material, an extensive crust, small rocks or clods which seem to be difficult to collect, and more extensive erosion by the retro-engine exhaust gases than lander 1. A report on the physical properties of the martian surface based on data obtained through sol 58 on Viking 2 and a brief description of activities on Viking 1 after sol 36 are given.*

This report is primarily concerned with Viking 2 lander (VL2) data; however, some of the results obtained on Viking 1 after sol 36 will be reported. Earlier reports (1, 2) on the "soil" (3) properties of Mars were based on data obtained during the first 36 sols (4) of Viking 1 lander (VL1).

The dynamics of both landings were similar—an almost vertical descent during the last 10 seconds and a "soft" touchdown—but minor variations occurred. The activities of the surface sampler on VL2 were also similar to those carried out on VL1 with the addition that samples were obtained from under rocks for the biology and gas chromatograph-mass spectrometer (GCMS) experiments.

The surface materials in the sample field at Utopia Planitia can be described as blocks and fragments set in a matrix of finer-grained material (Figs. 1–3). Beyond the sample field, small dunes (pitted by rocks propelled by the engine exhausts) indicate a local wind direction near 320° . Blocks within the sample field attain dimensions of 0.65 by 0.23 m. Because of the viewing angles, the third dimension of blocks normally cannot be measured and much of the interblock surface is obscured. Finer-grained materials between rocks and fragments are present as fillets, small drifts, a weak platy crust, and subcrust materials; small clods and rock fragments are abundant everywhere between the rocks. Unlike the VL1 site at Chryse where the sample field could be divided into an area underlain by very fine-grained material and a rocky area (1, 2), Utopia Planitia is more uniform. The sample field at Utopia Planitia near footpad 3 and the ejected shroud are relatively rock-free, but materials there

appear similar to those elsewhere (Fig. 2).

Deposits of cross-bedded drifts superposed on a rocky substrate, which covered extensive areas at the VL1 site, are virtually absent at Utopia Planitia. The rocky, deflated appearance of the VL2 site is consistent with orbital images of the site, in particular, and the region from 44°N to 48°N in general. Orbital images of the northern latitudes show partially stripped lava flows and ejecta blankets, hexagonal to reticulate structural patterns enhanced by erosion and deflation, secondary craters standing in stark relief because of deflation, and deflation hollows. These features are found in the general area of the VL2 landing site. There is no evidence for a thick aeolian mantle of fines or dune deposits as had been expected by many members of the landing site selection team.

Touchdown. Landing conditions for both VL1 and VL2 were close to nominal, with the exception of an anomaly which occurred during the last 0.4 second of the VL2 decent when there was a sudden reduction in the velocity at touchdown. Nominal conditions during the last 10 seconds before landing are vertical descent at a constant velocity of 2.44 m/sec and a horizontal attitude controlled by the lander radar and guidance system. The thrust of the descent engines is terminated upon contact of the footpads with the surface. The time interval between surface contact and the beginning of thrust decay is about 20 msec, and the decay time constant is about 30 msec. Touchdown parameters are given in Table 1.

The average leg stroke on VL1 was larger than on VL2. These data were at first surprising because both landers nominally appeared to have the same ki-